

The η^4 -*o*-Benzoquinone Manganese Tricarbonyl Anion (*o*-QMTC) as an Organometallogand in the Formation of $M(o\text{-QMTC})_2(L-L)$ Complexes ($M = \text{Mn, Co, Cd}$; $L-L = \text{bipy, phen}$): Generation of Neutral 2-D Networks Containing Two Types of $\pi-\pi$ Stacking

Moonhyun Oh, Gene B. Carpenter, and D. A. Sweigart*

Department of Chemistry, Brown University, Providence, Rhode Island 02912

Received January 7, 2003

The complex $(\eta^6\text{-catechol})\text{Mn}(\text{CO})_3^+$ is readily deprotonated to $(\eta^4\text{-}o\text{-benzoquinone})\text{Mn}(\text{CO})_3^-$ (*o*-QMTC), which functions as an organometallogand toward divalent metal ions by σ -bonding through the quinone oxygen atoms. The ligand *o*-QMTC, together with 2,2'-bipyridine or 1,10-phenanthroline ($L-L$), was found to produce the stable complexes $M(o\text{-QMTC})_2(L-L)$ ($M = \text{Mn, Co, Cd}$). Crystal structures of $\text{Mn}(o\text{-QMTC})_2(\text{bipy})$, $\text{Co}(o\text{-QMTC})_2(\text{bipy})$, and $\text{Cd}(o\text{-QMTC})_2(\text{phen})$ revealed in each case a two-dimensional supramolecular architecture consisting of $\pi-\pi$ stacking and interdigitation of the bipy or phen ligands, as well as a pairwise $\pi-\pi$ stacking of one of the two benzoquinone rings in each monomeric unit to generate dimeric units.

Introduction

When dihydroxybenzenes (hydroquinones) are η^6 -coordinated to the $\text{Mn}(\text{CO})_3^+$ moiety, the $-\text{OH}$ protons become quite acidic and the complexes are easily deprotonated with mild base to afford semiquinone and quinone complexes, respectively. Scheme 1 illustrates this process with the η^6 π -coordinated complex of *o*-dihydroxybenzene (catechol). Note that the deprotonation sequence **1a** (η^6) \rightarrow **1b** (η^5) \rightarrow **1c** (η^4) is formally equivalent to the well-known and important proton-coupled oxidation of catechol to *o*-benzosemiquinone and *o*-benzoquinone, also shown in Scheme 1. In this context, the $\text{Mn}(\text{CO})_3$ moiety acts as an internal oxidant that accepts an electron upon each deprotonation. Thus, it may be argued that metal coordination facilitates both proton and electron loss.

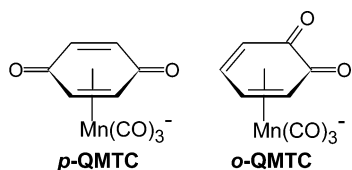
Thermally stable η^6 π complexes of dihydroxybenzenes are easily synthesized in high yield by reacting the arene with the manganese tricarbonyl transfer reagent $(\eta^6\text{-naphthalene})\text{Mn}(\text{CO})_3^+$.^{1,2} In the case of 1,4-dihydroxybenzene (hydroquinone), we previously demonstrated that the η^4 -quinone anion obtained by double deprotonation ("*p*-QMTC") functions as a good ligand

("organometallogand") toward divalent transition-metal ions to give polymeric metal-organometallic coordination networks (MOMNs).³ The para disposition of the quinone oxygen atoms in *p*-QMTC requires that each oxygen σ -binds to a different metal, thus accounting for the formation of polymers. With the *o*-QMTC isomer derived from catechol, both oxygen atoms can σ -bind to the same metal center, so that monomeric products may be formed.

Herein we report that *o*-QMTC reacts with divalent metal ions (Mn^{2+} , Co^{2+} , Cd^{2+}) in the presence of 2,2'-bipyridine (bipy) or 1,10-phenanthroline (phen) to form the neutral metal-organometallic complexes **2–5** of general formula $M(o\text{-QMTC})_2(L-L)$, in which *o*-QMTC acts as a chelating organometallogand. Chart 1 shows the formula key for the new compounds. X-ray studies of crystals of **2**, **3**, and **5** show that in the solid state all three compounds possess a similar and very interesting 2-D network structure consisting of two types of $\pi-\pi$ stacking interactions. One direction is defined by $\pi-\pi$ stacking of the bipy or phen ligands to produce molecular columns that are, in turn, linked via $\pi-\pi$ stacking of alternate quinone rings.

Results and Discussion

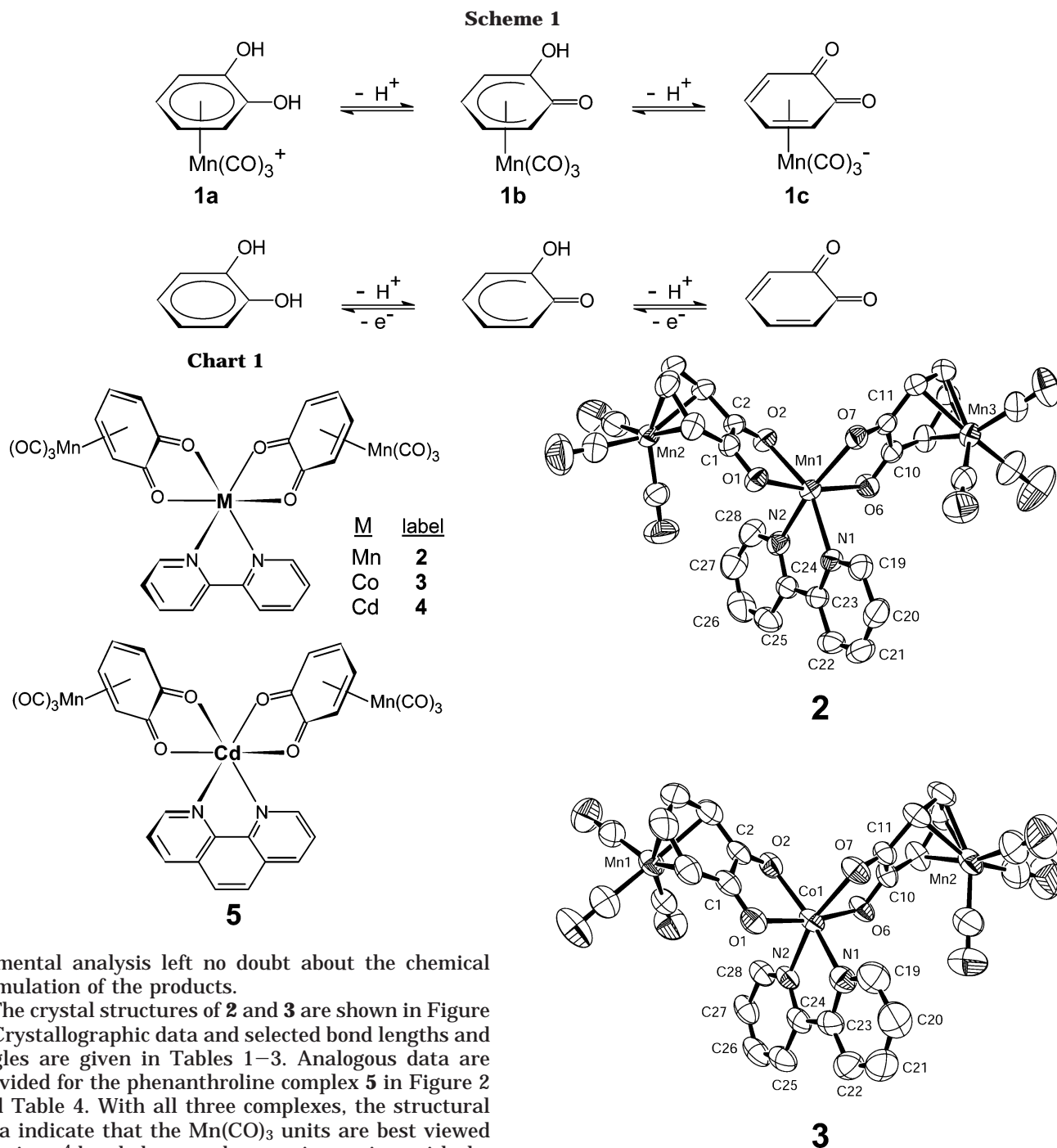
Complexes **2–5** were easily synthesized by combining the semiquinone complex **1b** with the appropriate metal acetate in $\text{MeOH}/\text{CH}_2\text{Cl}_2$ solvent containing 1 equiv of bipy or phen. In this procedure, the acetate anion functions as a base to deprotonate **1b** in situ to afford the quinone organometallogand **1c**. IR, NMR, MS, and



(1) (a) Sun, S.; Yeung, L. K.; Sweigart, D. A.; Lee, T.-Y.; Lee, S. S.; Chung, Y. K.; Switzer, S. R.; Pike, R. D. *Organometallics* **1995**, *14*, 2613. (b) Sun, S.; Carpenter, G. B.; Sweigart, D. A. *J. Organomet. Chem.* **1996**, *512*, 257.

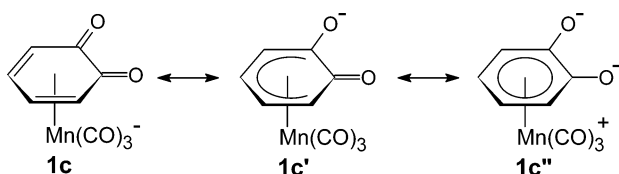
(2) Oh, M.; Carpenter, G. B.; Sweigart, D. A. *Organometallics* **2002**, *21*, 1290.

(3) (a) Oh, M.; Carpenter, G. B.; Sweigart, D. A. *Angew. Chem., Int. Ed.* **2001**, *40*, 3191. (b) Oh, M.; Carpenter, G. B.; Sweigart, D. A. *Angew. Chem., Int. Ed.* **2002**, *41*, 3650. (c) Oh, M.; Carpenter, G. B.; Sweigart, D. A. *Chem. Commun.* **2002**, 2168.



elemental analysis left no doubt about the chemical formulation of the products.

The crystal structures of **2** and **3** are shown in Figure 1. Crystallographic data and selected bond lengths and angles are given in Tables 1–3. Analogous data are provided for the phenanthroline complex **5** in Figure 2 and Table 4. With all three complexes, the structural data indicate that the $\text{Mn}(\text{CO})_3$ units are best viewed as being η^4 -bonded to an σ -benzoquinone ring, with the average Mn–C diene distance being 2.16 Å. The other ring carbon atoms (C(1), C(2) or C(10), C(11)) are much farther from the manganese at an average of 2.5 Å. This distance, however, is short enough to indicate some bonding interaction with the metal, which, in turn, implies a contribution from the η^5 and η^6 resonance forms **1c'** and **1c''**. The interplanar angle between the



dioxo part of the carbocyclic ring, C(3)–C(2)–C(1)–C(6), and the diene part, C(3)–C(4)–C(5)–C(6), averages

Figure 1. Crystal structures of **2** and **3** with the thermal ellipsoids at the 50% probability level.

about 10° in **2**, **3**, and **5**. This is a value much less than that found⁴ in $(\eta^4\text{-naphthalene})\text{Mn}(\text{CO})_3^-$, a fact also suggestive of a contribution from the resonance forms **1c'** and **1c''**. This behavior is akin to “valence tautomerism” or “redox isomerization” described by Pierpont⁵ for catecholate complexes containing a metal σ -bonded to the oxygen atoms. The Pierpont work demonstrated facile intramolecular electron transfer between the metal and the organic quinone system, and this was

(4) Thompson, R. L.; Lee, S.; Rheingold, A. L.; Cooper, N. J. *Organometallics* **1991**, *10*, 1657.

(5) (a) Pierpont, C. G.; Langi, C. W. *Prog. Inorg. Chem.* **1994**, *41*, 331. (b) Pierpont, C. G. *Coord. Chem. Rev.* **2001**, *216–217*, 99.

Table 1. Crystallographic Data for Complexes 2, 3, and 5

	2	3	5
formula	C ₂₈ H ₁₆ Mn ₃ N ₂ O ₁₀	C ₂₈ H ₁₆ CoMn ₂ N ₂ O ₁₀	C ₃₀ H ₁₆ CdMn ₂ N ₂ O ₁₀
fw	705.25	709.24	786.73
temp, K	298	298	298
wavelength, Å	0.710 73	0.710 73	0.710 73
cryst syst	triclinic	triclinic	triclinic
space group	<i>P</i> 1	<i>P</i> 1	<i>P</i> 1
<i>a</i> , Å	7.2344(4)	7.3283(7)	7.2304(4)
<i>b</i> , Å	15.0305(8)	14.2772(13)	12.4676(6)
<i>c</i> , Å	15.5187(8)	15.4905(14)	16.2528(8)
α , deg	68.1120(10)	64.9180(10)	100.1870(10)
β , deg	87.5920(10)	87.551(2)	91.8930(10)
γ , deg	78.5130(10)	78.028(2)	97.7200(10)
<i>V</i> , Å ³	1533.48(14)	1434.1(2)	1426.53(13)
<i>Z</i>	2	2	2
<i>d</i> _{calcd} , g cm ⁻³	1.527	1.642	1.832
μ , mm ⁻¹	1.272	1.499	1.674
<i>F</i> (000)	706	710	776
crystal dimens, mm	0.30 × 0.23 × 0.17	0.26 × 0.08 × 0.03	0.18 × 0.08 × 0.05
θ range, deg	2.41–26.39	2.59–26.41	2.55–28.29
no. of rflns collected	14 586	13 567	15 564
no. of indep rflns	6202 (<i>R</i> _{int} = 0.0194)	5821 (<i>R</i> _{int} = 0.0616)	6935 (<i>R</i> _{int} = 0.0301)
no. of data/restraints/params	6202/0/388	5821/0/388	6935/0/406
GOF on <i>F</i> ²	1.074	0.968	1.006
<i>R</i> 1, <i>wR</i> 2 (<i>I</i> > 2 σ (<i>I</i>))	0.0334, 0.0867	0.0580, 0.1015	0.0410, 0.0841
<i>R</i> 1, <i>wR</i> 2 (all data)	0.0390, 0.0893	0.1393, 0.1248	0.0656, 0.0931

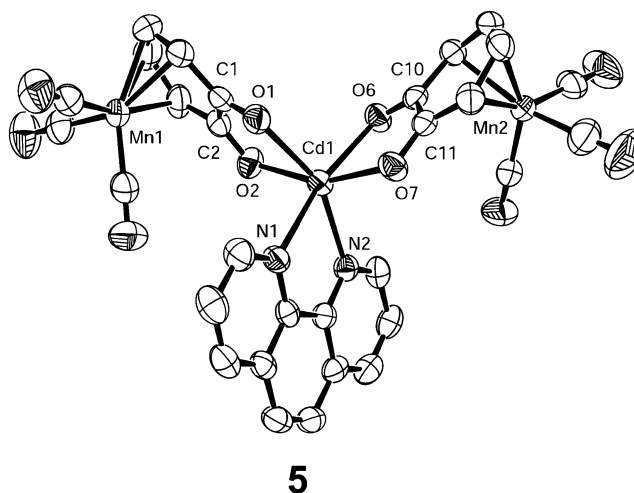
Table 2. Selected Bond Distances (Å) and Angles (deg) for Complex 2

Mn(1)–O(1)	2.1536(13)	Mn(1)–O(2)	2.1927(13)
Mn(1)–O(6)	2.1509(14)	Mn(1)–O(7)	2.2098(13)
Mn(1)–N(1)	2.2491(16)	Mn(1)–N(2)	2.2461(17)
Mn(2)–C(1)	2.5172(18)	Mn(2)–C(2)	2.5360(19)
Mn(2)–C(3)	2.213(2)	Mn(2)–C(4)	2.121(2)
Mn(2)–C(5)	2.109(2)	Mn(2)–C(6)	2.212(2)
Mn(3)–C(10)	2.4841(19)	Mn(3)–C(11)	2.4702(19)
Mn(3)–C(12)	2.192(2)	Mn(3)–C(13)	2.113(2)
Mn(3)–C(14)	2.123(2)	Mn(3)–C(15)	2.220(2)
C(1)–O(1)	1.268(2)	C(2)–O(2)	1.269(2)
C(10)–O(6)	1.268(2)	C(11)–O(7)	1.267(2)
O(1)–Mn(1)–O(2)	76.16(5)	O(6)–Mn(1)–O(7)	75.50(5)
C(1)–O(1)–Mn(1)	113.65(12)	C(2)–O(2)–Mn(1)	112.31(11)
C(10)–O(6)–Mn(1)	113.70(12)	C(11)–O(7)–Mn(1)	111.48(11)
N(2)–Mn(1)–N(1)	72.33(6)		

Table 3. Selected Bond Distances (Å) and Angles (deg) for Complex 3

Co(1)–O(1)	2.051(4)	Co(1)–O(2)	2.142(4)
Co(1)–O(6)	2.077(3)	Co(1)–O(7)	2.105(3)
Co(1)–N(1)	2.104(5)	Co(1)–N(2)	2.111(4)
Mn(1)–C(1)	2.469(6)	Mn(1)–C(2)	2.484(6)
Mn(1)–C(3)	2.192(5)	Mn(1)–C(4)	2.117(5)
Mn(1)–C(5)	2.123(5)	Mn(1)–C(6)	2.223(5)
Mn(2)–C(10)	2.513(5)	Mn(2)–C(11)	2.541(5)
Mn(2)–C(12)	2.209(5)	Mn(2)–C(13)	2.114(6)
Mn(2)–C(14)	2.113(6)	Mn(2)–C(15)	2.214(5)
C(1)–O(1)	1.265(6)	C(2)–O(2)	1.256(6)
C(10)–O(6)	1.267(5)	C(11)–O(7)	1.259(5)
O(1)–Co(1)–O(2)	78.60(14)	O(6)–Co(1)–O(7)	79.41(13)
C(1)–O(1)–Co(1)	112.3(3)	C(2)–O(2)–Co(1)	109.4(3)
C(10)–O(6)–Co(1)	111.6(3)	C(11)–O(7)–Co(1)	110.3(3)
N(1)–Co(1)–N(2)	76.94(18)		

suggested to occur because relevant metal and ligand orbitals are close in energy. As would be expected, the degree of electron transfer was found to be temperature dependent, implying that certain chemical and physical properties may be tunable to a degree. In the case of complexes **2–5**, there are metals both σ -bonded and π -bonded to the quinone system, and there is evidence that the π -bonded metal can play an important role as an “electron sink” (vide infra).

**Figure 2.** Crystal structure of **5** with the thermal ellipsoids at the 50% probability level.**Table 4. Selected Bond Distances (Å) and Angles (deg) for Complex 5**

Cd(1)–O(1)	2.332(2)	Cd(1)–O(2)	2.255(2)
Cd(1)–O(6)	2.293(2)	Cd(1)–O(7)	2.242(2)
Cd(1)–N(1)	2.341(3)	Cd(1)–N(2)	2.343(3)
Mn(1)–C(1)	2.513(4)	Mn(1)–C(2)	2.512(3)
Mn(1)–C(3)	2.211(4)	Mn(1)–C(4)	2.116(4)
Mn(1)–C(5)	2.116(4)	Mn(1)–C(6)	2.204(4)
Mn(2)–C(10)	2.536(3)	Mn(2)–C(11)	2.516(3)
Mn(2)–C(12)	2.212(4)	Mn(2)–C(13)	2.112(3)
Mn(2)–C(14)	2.116(3)	Mn(2)–C(15)	2.203(4)
C(1)–O(1)	1.264(4)	C(2)–O(2)	1.259(4)
C(10)–O(6)	1.260(4)	C(11)–O(7)	1.262(4)
O(2)–Cd(1)–O(1)	73.12(8)	O(7)–Cd(1)–O(6)	73.60(8)
C(1)–O(1)–Cd(1)	111.5(2)	C(2)–O(2)–Cd(1)	114.4(2)
C(10)–O(6)–Cd(1)	112.15(19)	C(11)–O(7)–Cd(1)	114.2(2)
N(1)–Cd(1)–N(2)	71.37(9)		

The most interesting structural aspect of **2–5** concerns intermolecular π – π interactions, revealed by the crystal structure determinations. These interactions were found to be very similar in all three structures, and for this reason only those in complex **2** are il-

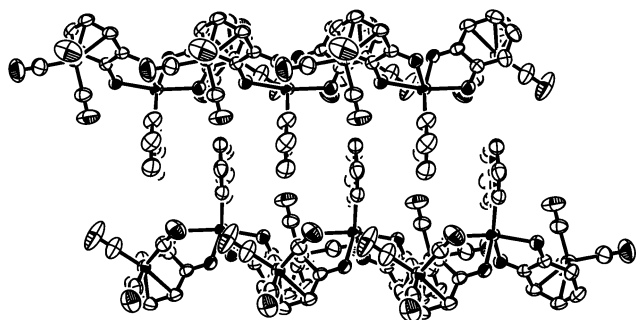


Figure 3. Bipyridine π - π stacking in complex **2**.

illustrated and discussed in detail. Figure 3 shows how the coordinated bipyridine ligands in **2** interdigitate via π - π stacking to generate one-dimensional arrays. Such π - π stacking of coordinated and uncoordinated pyridine type ligands is well documented for simple coordination complexes.^{5b,6} In **2** and **5** the stacked bipyridine or phenanthroline ring-to-ring separation is very short at only 3.3 Å, and in the cobalt complex **3** the separation is nearly as short at 3.4 Å. Additionally, the solid-state structure shows that the one-dimensional bipyridine arrays in Figure 3 are further assembled into the interesting two-dimensional structure shown in Figure 4. An examination of the crystal structure reveals the presence of π -stacking interactions involving the coordinated benzoquinone ligands. It is these novel interactions that are responsible for linking together the individual one-dimensional π -stacked bipyridine arrays to generate the two-dimensional network shown.

Figure 5 shows a "top" view of the two-dimensional network that defines the structure of complexes **2**–**5**. It is apparent that the coordinated benzoquinone rings are π - π stacked. The ring-to-ring distance is very short at 3.1 Å for **2** and **3** and 3.2 Å for **5**. As would be expected for a π - π interaction, the stacked quinone rings are offset, rather than eclipsed. Unlike the bipyridine–bipyridine interactions, which produce an interdigitated structure, the quinone–quinone interactions occur pairwise. One such pair for complex **2** is shown in Figure 6. The π - π stacking is clearly illustrated by the space-filling model in Figure 6. There is no contribution from an edge-to-face interaction.⁷

One can view the structures of **2**–**5** as consisting of dimeric units analogous to that shown in Figure 6, which subsequently undergo stacking via the bipyridines to generate the observed architecture. (Which type of π -stacking occurs "first" may not be a meaningful question.) A consequence of the quinone–quinone stacking is the presence of two types of $\text{Mn}(\text{CO})_3$ moieties, one bonded to a π -stacked quinone and one not so bonded. In accordance with this, IR spectra in KBr show two sets of tricarbonyl ν_{CO} bands, whereas in solution only one set is observed. For example, complex **2** has sets of ν_{CO} bands at 2029, 1962, 1945 cm^{-1} and 2009,

1926, 1916 cm^{-1} in the solid state. We associate the lower frequency set with the π -stacked quinone, in accordance with expectations based on published IR frequencies of metal–organometallic coordination polymers based on *p*-benzoquinone.³ In support of this assignment, the interplanar angle made by the diene carbons and the C_2O_2 part of the quinone is several degrees larger for the quinone participating in π -stacking compared to the other. As discussed above, a larger angle is expected to correlate with greater electron density on the metal and hence lower frequency ν_{CO} bands.

Conclusions

It has been demonstrated that $(\eta^4\text{-}o\text{-benzoquinone})\text{-Mn}(\text{CO})_3^-$ (*o*-QMTC) functions as a chelating organometallogand toward divalent metal ions. With 2,2'-bipyridine or 1,10-phenanthroline as coligands, stable neutral complexes with the formula $\text{M}(\text{o-QMTC})_2\text{-}(\text{L-L})$ are formed. In the solid state these complexes self-assemble into two-dimensional supramolecular networks, the structures of which are determined by (1) π - π stacking and interdigitation of the bipyridine or phenanthroline ligands and by (2) a pairwise π - π stacking of one of the two benzoquinone ligands in each monomeric unit to generate dimeric units. Modular organometallic units that self-assemble into supramolecular structures, whether the driving force is hydrogen bonding,⁸ metal–ligand σ -bond formation,³ or π - π stacking as herein, are of much interest in the more general context of supramolecular chemistry.⁹ The redox-active nature of σ -bonded benzoquinone complexes⁵ coupled with the electron sink nature of the $\text{Mn}(\text{CO})_3$ moiety in π -bonded benzoquinone complexes suggests that complexes containing organometallogands *o*-QMTC and *p*-QMTC may possess interesting and useful properties that reflect a self-adjusting electronic environment at the σ -bonded metal. Relevant studies are underway to examine this.

Experimental Section

General Considerations. Standard materials were purchased from commercial sources and used without further purification. Methanol and dichloromethane solvents were HPLC grade and were opened under nitrogen. ^1H and ^{13}C NMR spectra were recorded on Bruker 300 and 400 MHz instruments. Literature methods¹ were used to synthesize $[(\eta^6\text{-catechol})\text{Mn}(\text{CO})_3]\text{BF}_4$ (**1a**) and $(\eta^5\text{-}o\text{-semiquinone})\text{-Mn}(\text{CO})_3$ (**1b**).

$\text{Mn}(\text{o-QMTC})_2(\text{bipy})$ (2**).** The complex $(\eta^5\text{-}o\text{-semiquinone})\text{-Mn}(\text{CO})_3$ (**1b**; 20 mg, 0.08 mmol) and $\text{Mn}(\text{OAc})_2$ (10 mg, 0.04 mmol) were combined in $\text{MeOH}/\text{CH}_2\text{Cl}_2$ cosolvent in the presence of bipy (15 mg, 0.10 mmol) at room temperature.

(8) (a) Braga, D.; Grepioni, F.; Desiraju, G. R. *Chem. Rev.* **1998**, *98*, 1375. (b) Braga, D.; Grepioni, F. *Coord. Chem. Rev.* **1999**, *183*, 19. (c) Braga, D.; Maini, L.; Grepioni, F.; Elschenbroich, C.; Paganelli, F.; Schiemann, O. *Organometallics* **2001**, *20*, 1875. (d) Fraser, C. A. S.; Jenkins, H. A.; Jennings, M. C.; Puddephatt, R. J. *Organometallics* **2000**, *19*, 1635.

(9) (a) Lehn, J. M. *Supramolecular Chemistry: Concepts and Perspectives*; VCH: Weinheim, Germany, 1995. (b) Steed, J. W.; Atwood, J. L. *Supramolecular Chemistry*; Wiley: Chichester, U.K., 2000. (c) Holliday, B. J.; Mirkin, C. A. *Angew. Chem., Int. Ed.* **2001**, *40*, 2022. (d) Moulton, B.; Zaworotko, M. J. *Chem. Rev.* **2001**, *101*, 1629. (e) Robson, R. *J. Chem. Soc., Dalton Trans.* **2000**, 3735. (f) Fujita, M. *Chem. Soc. Rev.* **1998**, *27*, 417. (g) Claessens, C. G.; Stoddart, J. F. J. *Phys. Org. Chem.* **1997**, *10*, 254.

(6) (a) Yaghi, O. M.; Li, H.; Groy, T. L. *Inorg. Chem.* **1997**, *36*, 4292. (b) Domasevitch, K. V.; Enright, G. D.; Moulton, B.; Zaworotko, M. J. *J. Solid State Chem.* **2000**, *152*, 280. (c) Sommer, R. D.; Rheingold, A. L.; Goshe, A. J.; Bosnich, B. *J. Am. Chem. Soc.* **2001**, *123*, 3940. (d) Sun, W.-H.; Shao, C.; Chen, Y.; Hu, H.; Sheldon, R. A.; Wang, H.; Leng, X.; Jin, X. *Organometallics* **2002**, *21*, 4350.

(7) (a) Hunter, C. A.; Lawson, K. R.; Perkins, J.; Urch, C. J. *J. Chem. Soc., Perkin Trans. 2* **2001**, 651. (b) Rashkin, M. J.; Waters, M. L. *J. Am. Chem. Soc.* **2002**, *124*, 1860.

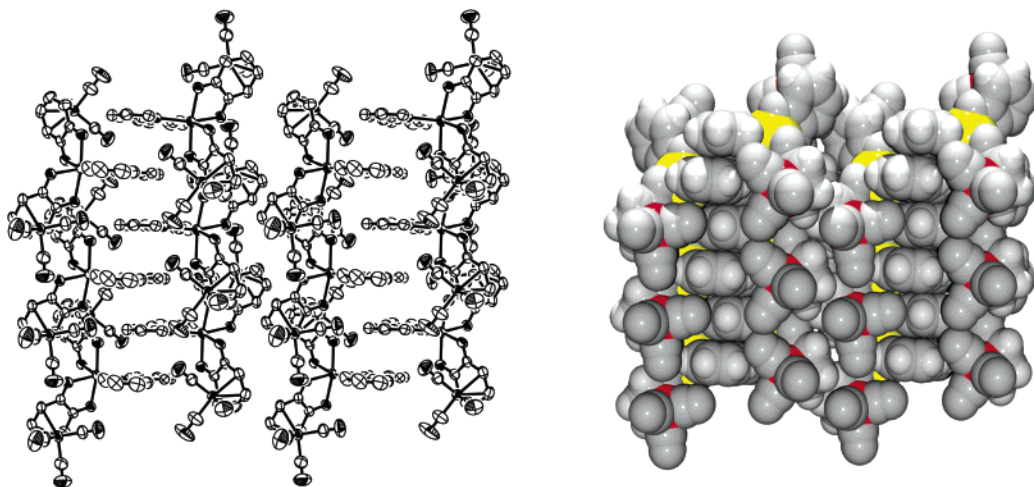


Figure 4. ORTEP and space-filling representations of the two-dimensional solid-state structure of complex **2**. The Mn(II) ions are in yellow.

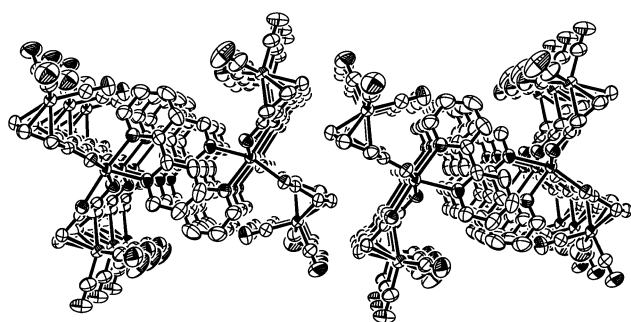


Figure 5. "Top" view of complex **2** showing π - π stacking of the benzoquinone ligands.

After slow evaporation of solvent at room temperature, crystals of complex **2** were obtained in 87% yield. IR (CH_2Cl_2): ν_{CO} 2026 (s) 1946 (s, br) cm^{-1} . IR (KBr): ν_{CO} 2029 (m), 2009 (s), 1962 (m), 1945 (s), 1926 (s), 1916 (s) cm^{-1} . FAB-MS: m/z 706 $[\text{M} + 1]^+$. Anal. Calcd for **2**, $\text{C}_{28}\text{H}_{16}\text{O}_{10}\text{N}_2\text{Mn}_3$: C, 47.69; H, 2.29; N, 3.97. Found: C, 47.46; H, 2.21; N, 3.90.

Co(o-QMTC)₂(bipy) (3). The cobalt analogue **3** was obtained in 77% yield by the same procedure as complex **2**, except that $\text{Co}(\text{OAc})_2$ replaced the $\text{Mn}(\text{OAc})_2$. IR (CH_2Cl_2): ν_{CO} 2026 (s) 1947 (s, br) cm^{-1} . IR (KBr): ν_{CO} 2028 (m), 2017 (s), 1962 (m), 1937 (s), 1926 (s), 1916 (s) cm^{-1} . FAB-MS: m/z 710 $[\text{M} + 1]^+$. Anal. Calcd for **3**, $\text{C}_{28}\text{H}_{16}\text{O}_{10}\text{N}_2\text{Mn}_2\text{Co}$: C, 47.42; H, 2.27; N, 3.95. Found: C, 47.45; H, 2.20; N, 3.88.

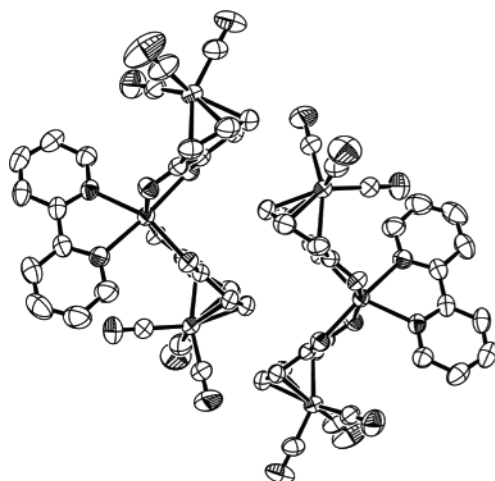
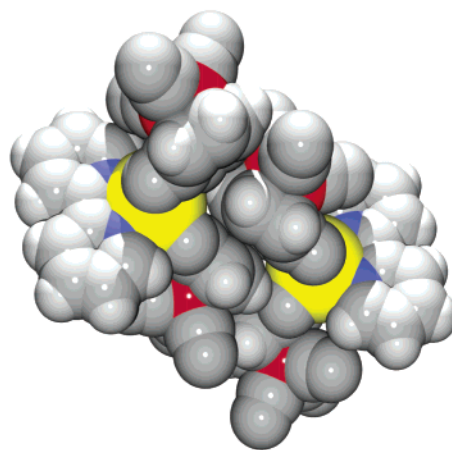


Figure 6. ORTEP and space-filling representations of the dimeric unit resulting from π -stacking of coordinated quinone ligands in complex **2**. The Mn(II) ions are in yellow.

Cd(o-QMTC)₂(bipy) (4). The cadmium analogue **4** was obtained in 84% yield by the same procedure as complex **2**, except that $\text{Cd}(\text{OAc})_2$ replaced the $\text{Mn}(\text{OAc})_2$. IR (CH_2Cl_2): ν_{CO} 2025 (s) 1944 (s, br) cm^{-1} . IR (KBr): ν_{CO} 2023 (m), 2015 (s), 1957 (m), 1949 (m), 1935 (s), 1927 (m) 1918 (s) cm^{-1} . ^1H NMR (CD_2Cl_2): δ 8.95 (br, 2H), 8.16 (br, 2H), 8.04 (br, 2H), 7.63 (br, 2H), 5.13 (dd, $J = 4.69$ Hz, $J = 3.55$ Hz, 4H), 4.97 (dd, $J = 4.69$ Hz, $J = 3.55$ Hz, 4H). ^{13}C NMR (CD_2Cl_2): δ 223.2 (Mn-CO), 161.0, 151.2, 149.8, 140.1, 126.3, 121.7, 85.3, 78.8. FAB-MS: m/z 763 $[\text{M} + 1]^+$. Anal. Calcd for **4**, $\text{C}_{28}\text{H}_{16}\text{O}_{10}\text{N}_2\text{Mn}_2\text{Cd}$: C, 44.09; H, 2.11; N, 3.67. Found: C, 43.89; H, 2.07; N, 3.59.

Cd(o-QMTC)₂(phen) (5). The cadmium analogue **5** was obtained in 88% yield by the same procedure as complex **2**, except that $\text{Cd}(\text{OAc})_2$ and phen replaced the $\text{Mn}(\text{OAc})_2$ and bipy. IR (CH_2Cl_2): ν_{CO} 2025 (s) 1944 (s, br) cm^{-1} . IR (KBr): ν_{CO} 2022 (s), 2013 (s), 1948 (m), 1935 (m), 1922 (s), 1915 (s) cm^{-1} . ^1H NMR (CD_2Cl_2): δ 9.24 (d, $J = 4.43$ Hz, 2H), 8.51 (d, $J = 7.73$ Hz, 2H), 7.97 (s, 2H), 7.92 (dd, $J = 7.73$ Hz, $J = 4.43$ Hz, 2H), 5.14 (m, $J = 3.68$ Hz, 4H), 5.00 (m, $J = 3.68$ Hz, 4H). Anal. Calcd for **5**, $\text{C}_{30}\text{H}_{16}\text{O}_{10}\text{N}_2\text{Mn}_2\text{Cd}$: C, 45.80; H, 2.05; N, 3.56. Found: C, 45.64; H, 1.98; N, 3.52.

Crystal Structures. Crystals of **2**, **3**, and **5** suitable for X-ray studies were grown from a solution of $\text{MeOH}/\text{CH}_2\text{Cl}_2$. X-ray data collection with Mo $\text{K}\alpha$ radiation was carried out at 298 K using a Bruker Apex diffractometer equipped with a CCD area detector. Structures were determined by direct methods and refined on F^2 . All hydrogen atoms were inserted in ideal positions, riding on their carbon atoms.



Acknowledgment is made to the donors of the Petroleum Research Fund, administered by the American Chemical Society, for support of this research.

Supporting Information Available: Tables of atomic coordinates, bond lengths and angles, anisotropic displacement

parameters, and hydrogen coordinates for **2**, **3**, and **5**. This material is available free of charge via the Internet at <http://pubs.acs.org>.

OM030009K